


Cross Talk between $\alpha 7$ and $\alpha 3\beta 4$ Nicotinic Receptors Prevents Their Desensitization in Human Chromaffin Cells

 Amanda Jiménez-Pompa,^{1,2} Sara Sanz-Lázaro,¹ Romidan Ewere Omodolor,¹ José Medina-Polo,³ Carmen González-Enguita,⁴ Jesús Blázquez,⁵ J. Michael McIntosh,^{6,7} and Almudena Albillos^{1,8}

¹Departamento de Farmacología y Terapéutica, Universidad Autónoma de Madrid, Madrid 28029, Spain, ²Instituto-Fundación Teófilo Hernando, Madrid 28029, Spain, ³Servicio de Urología, Hospital Universitario 12 de Octubre, Instituto de Investigación i+12, Madrid 28041, Spain, ⁴Servicio de Urología y Unidad de Trasplante Renal, Fundación Jiménez Díaz, Madrid 28040, Spain, ⁵Servicio de Urología, Hospital Clínico San Carlos, Madrid 28040, Spain, ⁶Departments of Biology and Psychiatry, University of Utah, Salt Lake City, UT 84108, ⁷George E. Wahlen Veterans Affairs Medical Center, Salt Lake City, UT 84108, and ⁸Instituto Ramón y Cajal de Investigación Biosanitaria (IRYCIS), Madrid 28034, Spain

The physical interaction and functional cross talk among the different subtypes of neuronal nicotinic acetylcholine receptors (nAChRs) expressed in the various tissues is unknown. Here, we have investigated this issue between the only two nAChRs subtypes expressed, the $\alpha 7$ and $\alpha 3\beta 4$ subtypes, in a human native neuroendocrine cell (the chromaffin cell) using electrophysiological patch-clamp, fluorescence, and Förster resonance energy transfer (FRET) techniques. Our data show that $\alpha 7$ and $\alpha 3\beta 4$ receptor subtypes require their mutual and maximal efficacy of activation to increase their expression, to avoid their desensitization, and therefore, to increase their activity. In this way, after repetitive stimulation with acetylcholine (ACh), $\alpha 7$ and $\alpha 3\beta 4$ receptor subtypes do not desensitize, but they do with choline. The nicotinic current increase associated with the $\alpha 3\beta 4$ subtype is dependent on Ca^{2+} . In addition, both receptor subtypes physically interact. Interaction and expression of both subtypes are reversibly reduced by tyrosine and serine/threonine phosphatases inhibition, not by Ca^{2+} . In addition, expression is greater in human chromaffin cells from men compared to women, but FRET efficiency is not affected. Together, our findings indicate that human $\alpha 7$ and $\alpha 3\beta 4$ subtypes mutually modulate their expression and activity, providing a promising line of research to pharmacologically regulate their activity.

Key words: $\alpha 3\beta 4$; $\alpha 7$; chromaffin cell; human; nicotinic receptor; patch-clamp

Significance Statement

Desensitization of nicotinic receptors is accepted to occur with repetitive agonist stimulation. However, here we show that human native $\alpha 3\beta 4$ and $\alpha 7$ nicotinic acetylcholine receptor (nAChR) subtypes do not desensitize, and instead, increase their activity when they are activated by the physiological agonist acetylcholine (ACh). An indispensable requirement is the activation of the other receptor subtype with maximal efficacy, and the presence of Ca^{2+} to cooperate in the case of the $\alpha 3\beta 4$ current increase. Because choline is an $\alpha 3\beta 4$ partial agonist, it will act as a limiting factor of nicotinic currents enhancement in the absence of ACh, but in its presence, it will further potentiate $\alpha 7$ currents.

Introduction

The main objective of the present study was to investigate whether $\alpha 7$ and non- $\alpha 7$ ($\alpha 3\beta 4$ in this study) nicotinic acetylcholine receptors (nAChRs) subtypes cooperate to drastically reduce their desensitization and increase their activity. Their

expression and physical interaction were also investigated, as well as their regulation by Ca^{2+} and kinases or phosphatases. These receptors are ligand-gated cationic channels that mediate fast synaptic transmission. There are different nicotinic receptor subunits, $\alpha 1$ – 7 , $\alpha 9$, $\alpha 10$, $\beta 1$ – $\beta 4$, γ , δ , and ϵ in mammals, which assemble into pentamers forming different heteromeric and homomeric subtypes. At least two nAChR subtypes are expressed in the different neuronal areas of the central and peripheral nervous systems. Whether they coexist to interact and mutually cooperate to regulate their activity has not been previously investigated in the native tissue. In *Xenopus* oocytes, a previous report by Criado et al. (2012) showed that $\alpha 7$ subunits possess the capacity to stably associate with $\beta 4$ or $\alpha 3$ subunits expressed. On the other hand, nAChRs exhibit desensitization, a characteristic kinetic property consisting of the loss of activity

Received May 24, 2021; revised Nov. 24, 2021; accepted Dec. 5, 2021.

Author contributions: A.J.-P., S.S.-L., and R.E.O. performed research; A.J.-P. analyzed data; A.J.-P., J.M.M., and A.A. wrote the paper; J.M.P., C.G.-E., J.B., and J.M.M. contributed unpublished reagents/analytic tools; A.A. designed research; A.A. wrote the first draft of the paper; A.A. edited the paper.

This work was supported by Spanish Ministerio de Ciencia y Tecnología Grants BFU2012-30997 and BFU2015-69092 (to A.A.) and National Institutes of Health Grants GM136430 and GM103801 (to J.M.M.).

The authors declare no competing financial interests.

Correspondence should be addressed to Almudena Albillos at almudena.albillos@uam.es.

<https://doi.org/10.1523/JNEUROSCI.1115-21.2021>

Copyright © 2022 the authors

with repetitive agonist stimulation. In particular, the $\alpha 7$ subtype forms homomeric receptors that exhibit a very fast desensitization process. Heteromeric $\alpha 7\beta 2$ receptors have also been reported, and show similar pharmacological sensitivities compared with the homomeric receptor. A decreased cholinergic activity has been reported for the $\alpha 7$ nAChR subtype in a number of pathologies such as Alzheimer's disease (AD). Therapeutic interventions aimed at reducing desensitization of this receptor subtype would be of great benefit for the treatment of these diseases.

We evaluated our hypothesis in the human chromaffin cell of the adrenal gland obtained from organ donors for the following reasons: (1) it expresses only two receptor subtypes, the $\alpha 7$ and $\alpha 3\beta 4$ subtypes (Pérez-Alvarez et al., 2012a,b; Hone et al., 2015, 2017), which makes easier to investigate physical and functional interactions; (2) it is a native system, which allows to better understand the physiological situation; and (3) it is a human cell, which avoids extrapolation from nonhuman species facilitating translation to human pathophysiology.

In this study, we have discovered key aspects of nAChRs physiology. After activation of both receptor subtypes with maximal efficacy, a population of nAChRs increases its expression at the plasma membrane, becomes activatable, and decreases its desensitization. Expression of these nAChR subtypes is regulated by phosphatases, as it is their physical interaction. We believe these data open a new line of research in the field of nAChRs and will help to find pharmacological tools to treat diseases in which the cholinergic function is impaired.

Materials and Methods

Reagents

ACh chloride, choline chloride, amphotericin B, penicillin/streptomycin, protease type XIV, collagenase type I, poly-D-lysine hydrobromide, red blood cell lysis solution, dimethylsulfoxide, bovine serum albumin (BSA), aprotinin, leupeptin trifluoroacetate, pepstatin A, 1,1-dimethyl-4-phenylpiperazinium iodide (DMPP), PNU-282987 (PNU) hydrate and all salts were purchased from Merck Sigma-Aldrich. DMEM, Glutamax, α -bungarotoxin Alexa Fluor 488 (BgTx-488) conjugate and ProLong Gold Antifade Mountant were purchased from ThermoFisher Scientific. Fetal bovine serum (FBS) was obtained from LabClinics.

Peptide synthesis

The α -conotoxin (α -Ctx) ArIB (V11,V16D; ArIB), was synthesized as previously described (Whiteaker et al., 2007). The α -Ctx TxID (TxID; Luo et al., 2013) was synthesized using an Apex 396 automated peptide synthesizer (AAPPTEC) according to previously described methods (Hone et al., 2013).

Cell culture of chromaffin cells

Human adrenal chromaffin cells were isolated and cultured as previously reported (Hone et al., 2015). Briefly, glands were perfused through the vein with protease type XIV and after dissecting the gland, the medullary tissue was extracted and digested by incubation with collagenase type I. Cells were isolated after several filtrations and plated on poly-L-lysine (0.1 mg/ml) coated coverslips. Cells were maintained in DMEM medium supplemented with 1% Glutamax, 10% FBS, and penicillin/streptomycin, at 37°C in an incubator under an atmosphere of 95% air and 5% CO₂ for up to 7 d. The culture medium was changed daily by exchanging ~70% of the solution with fresh medium.

Mouse chromaffin cells of C57/B6 mice were isolated and culture following the procedure previously reported by Pérez-Alvarez et al. (2011).

Electrophysiological recordings of "patch-clamp"

To perform the recordings of nicotinic currents in the perforated-patch configuration, the extracellular solution was: 2 mM CaCl₂, 145 mM NaCl, 5 mM KCl, 1 mM MgCl₂, 10 mM HEPES, and 10 mM glucose

(pH 7.4; 315 mOsm). When extracellular free-Ca²⁺ solutions were used, 5 mM EGTA was added to this solution in the absence of Ca²⁺. The composition of the intracellular solution was: 145 mM K-glutamate, 8 mM NaCl, 1 mM MgCl₂, 10 mM HEPES, and 0.5 mM amphotericin B (pH 7.2; 322 mOsm). ACh was applied at 300 μ M. An amphotericin B stock solution was prepared every day at a concentration of 50 mg/ml in dimethyl sulfoxide and kept protected from light. The final concentration of amphotericin B was prepared by the ultrasonication of 10 μ l of stock amphotericin B in 1 ml of internal solution in the darkness. Pipettes were tip-dipped in amphotericin-free solution for several seconds and back-filled with freshly mixed intracellular amphotericin solution.

The electrophysiological measurements were conducted using an EPC-10 USB amplifier and the PatchMaster program (HEKA Elektronik); 2- to 3-M Ω borosilicate glass polished pipettes were used. After the formation of the seal and the perforation, only those recordings with a leakage current below 20 pA were accepted. The series resistant values were 17.7 ± 3 and 16.3 ± 2 M Ω at the beginning and the end of the experiment, respectively ($n = 28$). Series resistance was compensated electronically up to 70% in the voltage-clamp mode. Cell membrane capacitance (C_m) changes as an index of exocytosis were estimated by the Lindau–Neher technique implemented in the Sine+DC feature of the PatchMaster lock-in software (Lindau and Neher, 1988). A 1-kHz, 70-mV peak-to-peak amplitude sinewave was applied at a holding potential (V_h) of -60 mV. The analysis of data was done using IGOR Pro software (WaveMetrics).

To conduct the experiments, cells were gravity perfused with the extracellular solution delivered through a polyethylene tube placed 10 μ m to the cell of interest. To ensure rapid solution exchange, a multi-barrel pipette was used for agonist delivery. Agonist pulses (500-ms pulses) were applied using a valve controller triggered by the amplifier. The extracellular solution without the agonist was perfused once the agonist application ended. The fluid level was continuously controlled by a home-made fiber optics system coupled to a pump that removed excess fluid.

Cell treatments

In the electrophysiological recordings and image experiments, ArIB and TxID were perfused at 100 and 300 nM, respectively, 5 min before and then during the whole protocol of the experiment. Okadaic acid (OA) was incubated for 24 h at 5 nM. Pervanadate (1 mM stock solution) was prepared daily by adding 50 μ l of H₂O₂ 0.3% at 950 μ l of orthovanadate 0.1 M and then used as a standard concentration of 50 μ M for 40 min. Genistein at 200 μ M was perfused for 10 min to evaluate its effect alone, or before the addition of pervanadate or OA, and then during the rest of the experiment.

The concentrations used for the different agonists and antagonists were chosen from previous studies performed in our laboratory in human chromaffin cells (Pérez-Alvarez and Albillos, 2007; Pérez-Alvarez et al., 2012a,b; Hone et al., 2015, 2017). Pervanadate and genistein conditions were taken from Charpentier et al. (2005). We tested different conditions for the OA (5, 10, and 20 nM) to find a concentration that provokes minimal cell death but sufficient effect on protein phosphatase (PP)2A. That range of concentrations was chosen to selectively target PP2A, given that higher concentrations also affect PP1.

Fluorescence

Cells plated on 12-mm glass coverslips were rinsed with PBS and then fixed with 2% paraformaldehyde (PFA) for 20 min. After that, three washing steps of 5 min with PBS were performed. Incubation of fluorescent labeled toxins was performed for 30–40 min on ice in a buffer containing 0.1 mg/ml BSA to block nonspecific binding and 10 μ g/ml each of aprotinin, leupeptin trifluoroacetate, and pepstatin A to prevent peptide degradation by proteases. This was followed by extensive wash-out with PBS. Finally, coverslips were mounted in ProLong, a liquid curing mountant applied to the microscope slides in direct contact with the cells of study, to protect fluorescent dyes from fading.

To study the interaction and expression of $\alpha 3\beta 4$ and $\alpha 7$ receptor subtypes, α -Ctx BuIA labeled with Cy3 (BuIA-Cy3; 300 nM), and BgTx-488 (1.2 μ M) were used, respectively. To define nonspecific binding,

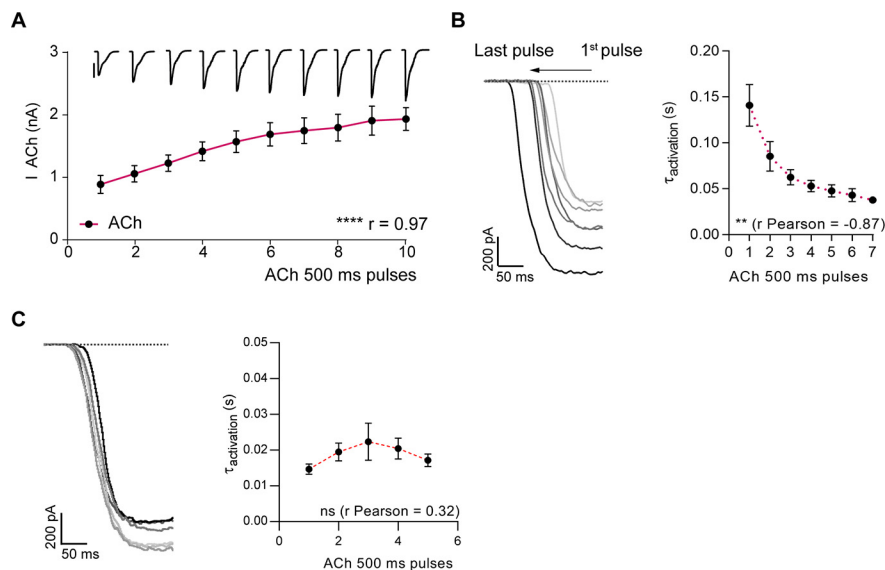


Figure 1. Repetitive pulses of ACh elicit an increase of nicotinic currents. **A**, Representation of the peak nAChR currents obtained at the first 10 ACh pulses (300 μ M, 500 ms, applied every 90 s), and their corresponding representative currents ($n = 8–12$). In one out of 29 cells, the increase of current did not occur. **B**, Left panel, The activation of the ACh currents plotted in panel **A** was enlarged to see in detail how currents exhibited faster activation with repetitive pulses. Right panel, Representation of the average activation time constant values ($\tau_{\text{activation}}$) of the nicotinic currents recorded at the first seven ACh pulses (number of pulses to reach the maximal ACh peak current; $n = 4–20$). **C**, The exchange of solutions in the perfusion system does not distort the activation kinetics of the nicotinic currents. Mouse chromaffin cells isolated and maintained in culture were used to perform these experiments. Repetitive pulses of ACh (300 μ M, 500-ms pulses applied every 90 s) were applied and the $\tau_{\text{activation}}$ of the nicotinic currents elicited by the first five ACh pulses plotted to show that very different responses are achieved using the same perfusion system. The first recorded current is drawn in gray and the successive currents are displayed with a gradient color until the last pulse that appears in black ($n = 23$). ** $p < 0.01$, **** $p < 0.0001$, ns $p > 0.05$.

control coverslips were treated with 2 nM nicotine 15 min before and during the fluorescent toxins incubation. As a negative control, some coverslips were labeled with only one fluorescent toxin. As an additional negative control, Förster resonance energy transfer (FRET) was also performed in nonchromaffin cells of the same coverslip, and in chromaffin cells of two-month-old mice in a different set of experiments, obtaining a FRET efficiency of zero in both cases (data not shown).

After performing FRET, the energy transfer efficiency could be quantified as:

$$\text{FRET}_{\text{eff}} = (D_{\text{post}} - D_{\text{pre}}) / D_{\text{post}}$$

where D_{pos} is the fluorescence intensity of the donor after acceptor photobleaching (AB), and D_{pre} the fluorescence intensity of the donor before AB. The FRET_{eff} is considered positive when $D_{\text{post}} > D_{\text{pre}}$ Hellenkamp et al. (2018).

Microscope image acquisition and analysis

Microscopy images were collected using a spectral confocal microscope (Leica TCS SP5) equipped with an argon laser (wavelength, 488 nm), DPSS laser (wavelength, 561 nm) and helium-neon laser (wavelengths, 594 and 633 nm) for the excitation of fluorescent probes. It has a 63 \times oil immersion objective with 1.4 of numerical aperture. Images were acquired in a medial plane (width of 0.772 μ m) in each cell under identical conditions to facilitate statistical analysis across conditions.

Expression of the different nAChR subtypes was determined by measuring the integrated density (IntDen), which is the product of the area and the mean gray value, by using Fiji-ImageJ software. Also, the Fiji-ImageJ colocalization Colormap plugin was used to calculate the colocalization correlation index values (I_{corr}). To perform and analyze FRET experiments, wizard AB (LAS AF, Leica) was used. The protocol consisted of 20 laser passes to bleach the acceptor (BuIA-Cy3). During the bleaching of the acceptor, only the 555 laser was on. The fluorescence of the donor (BgTx-488) was

measured with a 488 laser before and after AB. Only experiments in which AB was larger than 80% were considered for analysis. Red images were converted to magenta, to ensure legibility to color-blind people.

Experimental design and statistical analysis

The number of data n refers to the number of cells unless otherwise stated. Each experiment was performed in at least five donors. Data are given as mean \pm SEM. Statistical analysis was performed using IBM SPSS Statistics version 24.0. A Kolmogorov–Smirnov normality test was first performed. Then, paired or unpaired Student’s t test, Mann–Whitney’s U test, or Wilcoxon signed-rank tests were used and reported as t value and degrees of freedom, U value, sum of signed-ranks (W) and number of pairs, respectively. The exact p value was provided for each test. Differences were accepted as significantly different when the p value was under 0.05 (plot with an asterisk *), 0.01 (**), 0.001 (***), and 0.0001 (****). All the data values are shown in the dot plots.

Study approval

The human adrenal glands used in this study were collected from 30 organ donors (19 women and 11 men, from 23 to 82 years old) in three hospitals in Madrid (12 de Octubre, Fundación Jiménez Díaz, and Hospital Clínico San Carlos). Written consents were signed by donor’s relatives. The protocol was approved by the Ethics Committee of the Autonomous University of Madrid and by review boards of each hospital.

The mouse adrenal glands were collected from seven female C57/B6 mice two months old, provided by the animal facility of the Autonomous University of Madrid. All animals were housed on a 12/12 h light/dark cycle, with food and water *ad libitum*. All procedures used in this work were conducted according to the protocols approved by the Ethics Committee of the Autonomous University of Madrid and attention was put into ensuring that the animals experience the minimal suffering possible.

Results

Repetitive pulses of ACh elicit an increase of nicotinic currents

Repetitive pulses of ACh (300 μ M, 500 ms, applied every 90 s) elicited currents of increasing peak amplitude and charge. The r Pearson’s correlation coefficient was 0.97 ($R^2 = 0.9496$, $p < 0.0001$). The number of ACh pulses to reach the maximal increase of current was 7.1 ± 1.1 ($n = 29$; Fig. 1A). Initial peak current and charge values amounted to 813.1 ± 103.4 pA and 892.2 ± 176 pC ($n = 29$), respectively. After the application of ACh pulses, the maximal ACh peak current and charge increased to 1638 ± 167.8 pA ($W_{(29)} = -427$, $p < 0.0001$) and 1976 ± 318.7 pC ($W_{(29)} = -401$, $p < 0.0001$; $n = 29$), respectively, which normalized with respect to their own controls represents 2.1 \pm 0.2-fold and 2.5 \pm 0.3-fold of increment, respectively. The elicited-ACh currents exhibited faster activation kinetics with repetitive pulses, as shown by the representative traces and the activation time constant ($\tau_{\text{activation}}$) values in Figure 1B, left and right, respectively. Control experiments in mouse chromaffin cells were performed to exclude the possibility that the results in Figure 1B are an

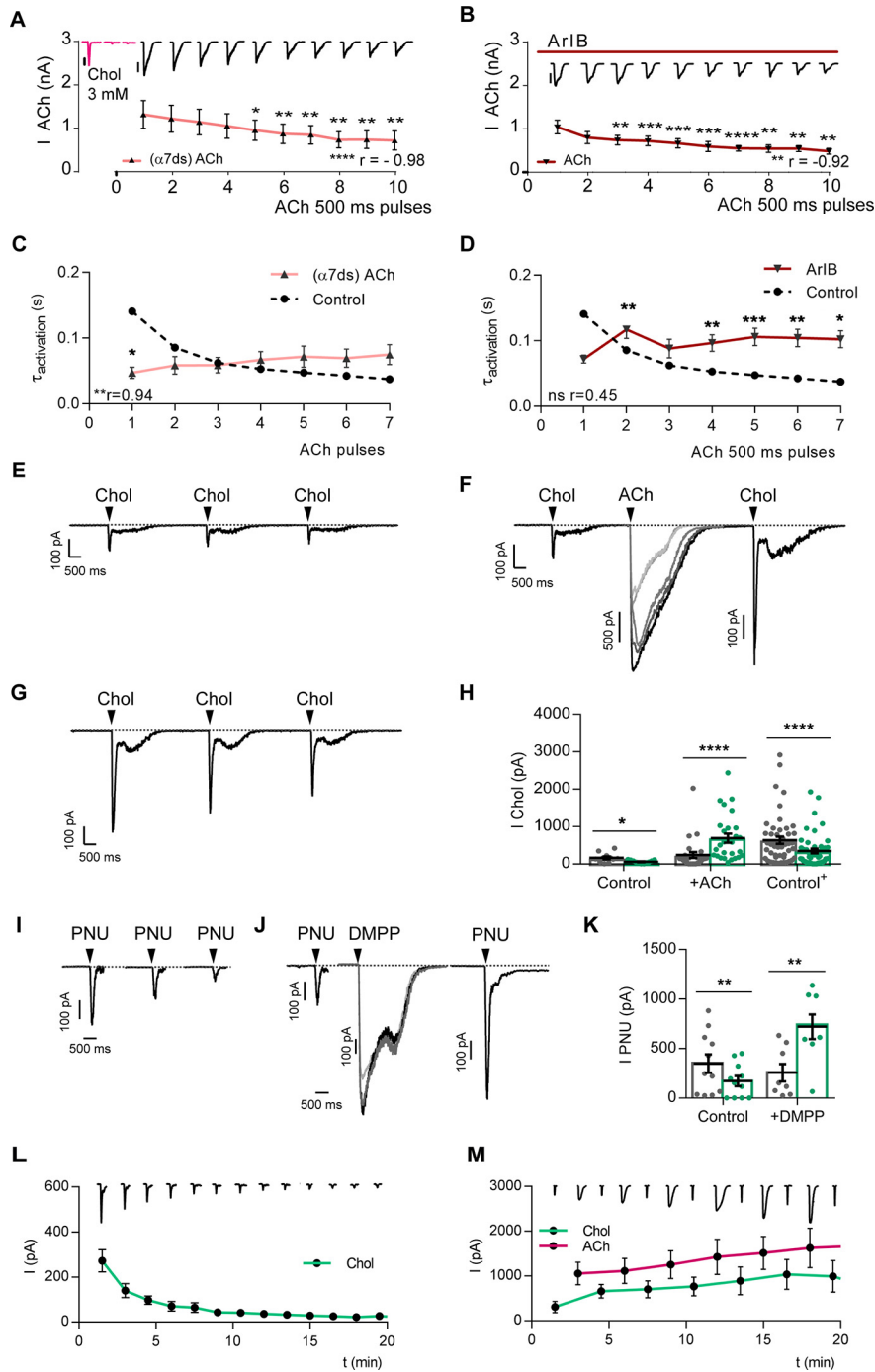


Figure 2. $\alpha 7$ and $\alpha 3\beta 4$ receptor subtypes require mutual and full activation to avoid their desensitization and to increase their activity. **A, B**, The ACh peak current is drawn with respect to the number of pulses under two different conditions. The corresponding representative recordings for each pulse are shown in the upper part of each panel. **A**, Desensitized $\alpha 7$ receptor condition ($\alpha 7$ ds): this receptor subtype was desensitized before starting the experiment by applying three pulses of choline (chol; 3 mM, 500 ms, applied every 90 s; $n = 7-10$). **B**, Blocked $\alpha 7$ receptor condition (ArIB): 100 nM ArIB was perfused for 5 min before the application of ACh pulses and then during the whole experiment ($n = 4-12$). Unpaired t test between each data point and its equivalent point in control conditions. ACh scale: 500 pA. Choline scale: 100 pA. **C, D**, $\tau_{\text{activation}}$ of the nicotinic currents from cells of panels **A, B** under the desensitized $\alpha 7$ receptor or ArIB conditions, in the seven successive ACh pulses. The dashed line represents the time constants of activation of the nicotinic currents from cells of Figure 1A, overlapped for ease of comparison. **E**, Representative recordings of three pulses of choline applied every 90 s (chol; 3 mM, 500 ms). **F**, First a pulse of choline was applied, then pulses of ACh were applied to fully activate $\alpha 7$ and $\alpha 3\beta 4$ receptor subtypes, and later on another choline pulse was applied again, obtaining larger choline-elicited currents. **G**, Once the $\alpha 7$ receptor potentiated currents were obtained, another two pulses of choline were applied every 90 s to observe whether the $\alpha 7$ receptor current is desensitized in the third pulse as it happened in panel **E**. **H**, A summary of the peak of the choline current elicited in the first (dark gray dots) and the third pulse (green dots) is drawn under control conditions (control), after the potentiation protocol (+ACh) and after desensitization of the $\alpha 7$ receptor potentiated currents (control+; $n = 11-48$). Paired t test. **I-K**, the same as in **E, F, H** (without control+), but

artifact of the perfusion system. Following the same protocol as in human cells, repetitive pulses of ACh elicited nicotinic currents with $\tau_{\text{activation}}$ values that do not exhibit faster activation kinetics. The r Pearson's correlation coefficient was 0.32 (ns, $n = 23$; Fig. 1C).

$\alpha 7$ and $\alpha 3\beta 4$ receptor subtypes require mutual and maximal efficacy of activation to avoid their desensitization and to increase their activity

In an additional set of experiments, we found that the increases of peak current achieved with repetitive ACh pulses were abolished if: (1) the $\alpha 7$ nicotinic current was desensitized previously at the beginning of the experiment by applying three pulses of 3 mM choline, an $\alpha 7$ receptor agonist; or (2) cells were perfused with the selective $\alpha 7$ receptor blocker ArIB (Whiteaker et al., 2007; Hone et al., 2015) at 100 nM during 5 min before the application of ACh pulses and then during the whole experiment. The protocol of these experiments was the same as that performed in Figure 1A. The graph of the ACh peak current at the different pulses and the corresponding representative recordings under both conditions, desensitizing previously the $\alpha 7$ receptor subtypes or after ArIB treatment, are drawn in Figure 2A,B, respectively. The r Pearson's correlation coefficients obtained were -0.98 ($R^2 = 0.9635$, $p < 0.0001$) and -0.92 ($R^2 = 0.8525$, $p = 0.0002$) for desensitized $\alpha 7$ receptor and ArIB conditions, respectively. Thus, the increase of current peak achieved with repetitive ACh pulses in control conditions was due in part to $\alpha 7$ receptor activation, since the observed changes were abolished in $\alpha 7$ desensitized receptors or ArIB-treated cells. On the other hand, the $\tau_{\text{activation}}$ of the nicotinic currents elicited with the successive ACh pulses in panels **A, B** are shown in Figure 2C,D, respectively. The r Pearson correlation coefficients were 0.94 ($R^2 = 0.8918$, $p = 0.0014$) and 0.45

using as agonists 30 μM PNU instead of choline and 100 μM DMPP instead of ACh ($n = 8-11$). Pulses of PNU and DMPP: 500 ms every 90 s. Paired t test. **L, M**, Time course of the peak currents elicited after application of successive choline pulses (**L**) or the choline pulses alternated with ACh pulses (**M**). Representative recordings are drawn in the upper part of both figures. The scale of the recordings and the time course is the same ($n = 6-15$). * $p < 0.05$, ** $p < 0.01$, *** $p < 0.001$, **** $p < 0.0001$, ns $p > 0.05$.

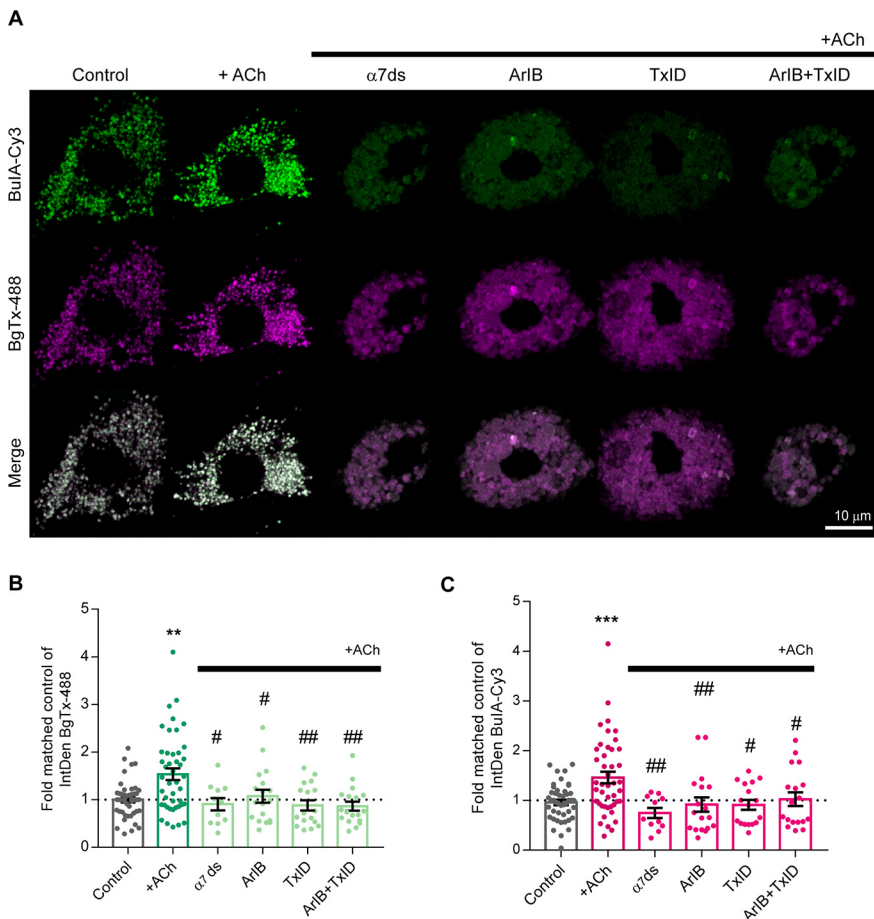


Figure 3. $\alpha 7$ and $\alpha 3\beta 4$ receptors require their mutual activation and to be in an active state to increase their expression. **A**, Representative fluorescent images of BgTx-488, BuIA-Cy3, and the resulting overlapping image (merge) obtained under different conditions: control; after the potentiation protocol (+ACh); after desensitization of the $\alpha 7$ receptor by applying three choline (3 mM) pulses every 90 s previously to the application of the potentiation protocol ($\alpha 7$ ds); after perfusion of 100 nM Ar1B (Ar1B), 300 nM Tx1D (Tx1D), or Ar1B and Tx1D 5 min before and during the application of the potentiation protocol. **B, C**, The corresponding fold times of increment of integrated density normalized with respect to its control was displayed for BgTx-488 and BuIA-Cy3, respectively ($n = 18-44$). Unpaired t test and Mann–Whitney test; *differences with respect to control; #differences with respect to +ACh. # $p < 0.05$, ## $p < 0.01$, ### $p < 0.001$.

($R = 0.1985$, $p = 0.3165$), respectively, for the desensitized $\alpha 7$ receptor and Ar1B conditions, respectively. This means that the recruitment of fast $\alpha 7$ receptors was essential for the decrease of the rate of activation observed in the control situation after repetitive ACh stimulation. Thus, during the repetitive stimulation with ACh $\alpha 7$ receptors not only do not desensitize but also activate faster and increase their amplitude.

However, the increase of currents cannot be attributed exclusively to $\alpha 7$ receptors recruitment, because the charge of the currents was also largely enhanced with successive agonist pulses. Therefore, activation of $\alpha 3\beta 4$ receptors is also increased, as it was later confirmed by the mutual requirement of their activation to obtain an increased expression of both receptor subtypes (see below). We posed the hypothesis that full and increased activation of $\alpha 3\beta 4$ receptors avoids $\alpha 7$ receptor desensitization, increasing their activity. We performed the experiments shown in Figure 2E,F to prove it. First, three pulses of 3 mM choline, an $\alpha 7$ receptor agonist that also activates non- $\alpha 7$ receptors in these cells (Pérez-Alvarez et al., 2012b), were applied successively every 90 s. The first peak of the current triggered by choline is because of $\alpha 7$ receptor stimulation, while the slow current activated after it is because of partial activation of non- $\alpha 7$ receptors (Pérez-Alvarez et al., 2012b; Hone et al.,

2015). Under that stimulation, a significant decrease of the choline peak current occurred. In these experiments, an initial peak current value of 164.2 ± 38.4 pA was decreased to 60.3 ± 12.6 pA. This corresponds to a decrease of $51.5 \pm 13.8\%$ in 11 cells tested ($t_{(10)} = 2.704$, $p = 0.0222$; Fig. 2E). However, if successive pulses of ACh were applied after the first choline pulse, and later on another choline pulse was applied again, the second choline pulse elicited now an increased peak current ($\alpha 7$ receptor potentiated currents; Fig. 2F). On average, peak currents increased from 242.2 ± 78.7 to 689.5 ± 119.1 pA after the ACh pulses. This meant a 2.8-fold increase in the 27 cells tested ($t_{(26)} = 4.696$, $p < 0.0001$). These $\alpha 7$ receptor potentiated currents could be again desensitized if repetitive pulses of choline were applied. Choline elicited currents now decreased from 636.3 ± 94.4 to 347.3 ± 63.3 pA, which represents a $45.3 \pm 4.8\%$ ($n = 48$; $t_{(47)} = 6.889$, $p < 0.0001$; Fig. 2G). All these data are summarized in the dot plot of Figure 2H. To search whether the same process occurs with a different $\alpha 7$ receptor agonist, 30 μ M PNU was perfused instead of choline, and the same protocol was performed. Three sequential PNU pulses caused a decrease of the peak current of $66.6 \pm 8.1\%$, from 348.3 ± 93.3 to 172.2 ± 51.4 pA ($n = 11$; $t_{(10)} = 3.989$, $p = 0.0026$; Fig. 2I). Also, a different $\alpha 3\beta 4$ and $\alpha 7$ agonist was now applied, DMPP, instead of ACh. The decrease of current triggered by PNU could be prevented if pulses of DMPP (100 μ M) were applied until the maximal current was achieved (5.2 ± 0.8 pulses).

PNU-elicited peak currents increased now from 256.8 ± 88.4 to 720.8 ± 123.8 pA. This corresponds to a 2.8-fold increase of the $\alpha 7$ receptor potentiated currents ($n = 8$; $t_{(7)} = 4.783$, $p = 0.002$; Fig. 2J). Data are summarized in the dot plot of Figure 2K. Thus, the $\alpha 7$ receptor subtype requires the activation of the $\alpha 3\beta 4$ receptor with full efficacy to avoid its desensitization.

Interestingly, the potentiation of the $\alpha 7$ receptor currents was a very rapid process since a single pulse of ACh was sufficient to avoid the $\alpha 7$ receptor desensitization and to induce the increase of the $\alpha 7$ current. As a control, we applied 13 choline pulses successively, decreasing the initial current from 271.9 ± 49.1 to 27 ± 14 pA ($n = 2-15$; 90% decrease; Fig. 2L). The Spearman's r correlation was -0.98 ($p < 0.0001$). However, when seven pulses of choline were alternatively applied with ACh pulses, the choline peak current increased its amplitude by 3-fold from 305.8 ± 127 pA ($n = 6$) to 992.3 ± 354.8 pA ($n = 3$). Also, the ACh elicited current increased from 1057.6 ± 255.7 pA ($n = 6$) to 1626.6 ± 441.3 pA ($n = 3$; 1.5-fold increase; Fig. 2M). The Spearman's r correlation between ACh and choline currents was 0.69 ($p < 0.0001$). These results reinforce the idea that activation with full efficacy of $\alpha 7$ and $\alpha 3\beta 4$ receptor subtypes is a requirement to increase their mutual activity.

$\alpha 7$ and $\alpha 3\beta 4$ receptors require their mutual activation and to be in an active state to increase their expression

We examined the variation of expression of $\alpha 7$ and $\alpha 3\beta 4$ receptor subtypes with repetitive pulses of ACh to evaluate whether it correlates with the activity of the channels. We used the BgTx-488 and BuIA-Cy3 to determine the expression of $\alpha 7$ and $\alpha 3\beta 4$ receptor subtypes, respectively. We can observe that the application of seven pulses of ACh (number of pulses required to achieve the maximal increase of ACh current) led to an increase of expression of both receptor subtypes (+ACh condition; Fig. 3A–C). We hypothesized that if the mutual activation of $\alpha 7$ and $\alpha 3\beta 4$ receptor subtypes avoids their desensitization leading to an increase of currents activation, it might well be that also the increase of expression of both receptor subtypes requires their mutual activation.

Different treatments were applied before stimulating the cell with seven pulses of ACh. These treatments included the application of three pulses of choline to desensitize the $\alpha 7$ receptor, the $\alpha 7$ receptor selective blocker ArIB, the $\alpha 3\beta 4$ receptor selective blocker TxID, or ArIB, and TxID simultaneously. The ArIB does not block non- $\alpha 7$ receptors ($\alpha 3\beta 2$, $\alpha 3\beta 4$, $\beta 3\alpha 6\beta 2\alpha 3\beta 4$ and $\alpha 6M211L$, $cyt\alpha 3\beta 4$) according to Hone et al. (2015). Besides, TxID does not block $\alpha 7$ receptor subtypes (Hone et al., 2017). Original fluorescence images are shown in Figure 3A and the summaries of the normalized integrated density of BgTx-488 and BuIA-Cy3 are plotted in Figure 3B,C, respectively. These experiments revealed that successive ACh pulses increased $\alpha 7$ and $\alpha 3\beta 4$ receptors expression by 1.5 ± 0.1 -fold ($U = 631$, $p = 0.0019$ and $t_{(87)} = 3.886$, $p = 0.0002$, respectively; $n = 44$). $\alpha 7$, and surprisingly, also $\alpha 3\beta 4$ receptor expression increases were abolished when $\alpha 7$ receptors were desensitized ($t_{(53)} = 2.457$, $p = 0.0173$ and $U = 100$, $p = 0.0021$, respectively; $n = 11$ with respect to ACh potentiated currents), or blocked with the selective $\alpha 7$ receptor antagonist ArIB ($t_{(60)} = 2.185$, $p = 0.0328$ and $U = 214$, $p = 0.0042$, respectively; $n = 18$). The increased expression of $\alpha 7$ or $\alpha 3\beta 4$ receptors was also prevented by the treatment of the cells with the $\alpha 3\beta 4$ receptor blocker TxID ($t_{(59)} = 3.123$, $p = 0.0028$ and $U = 218$, $p = 0.0114$, respectively; $n = 17$). When cells were treated with both toxins simultaneously, $\alpha 7$ and $\alpha 3\beta 4$ receptors' expression was not increased ($t_{(60)} = 3.323$, $p = 0.0015$ and $U = 256$, $p = 0.0296$, respectively; $n = 18$). These experiments reflect that $\alpha 7$ and $\alpha 3\beta 4$ receptor subtypes must be in an active, nondesensitized state to contribute to their increased expression and also to the expression of the other receptor subtype.

Dependence of Ca^{2+} of the ACh-evoked nicotinic current increment

The increase of the ACh peak currents shown under control conditions in Figure 1A is reduced in the absence of Ca^{2+} (Fig. 4A).

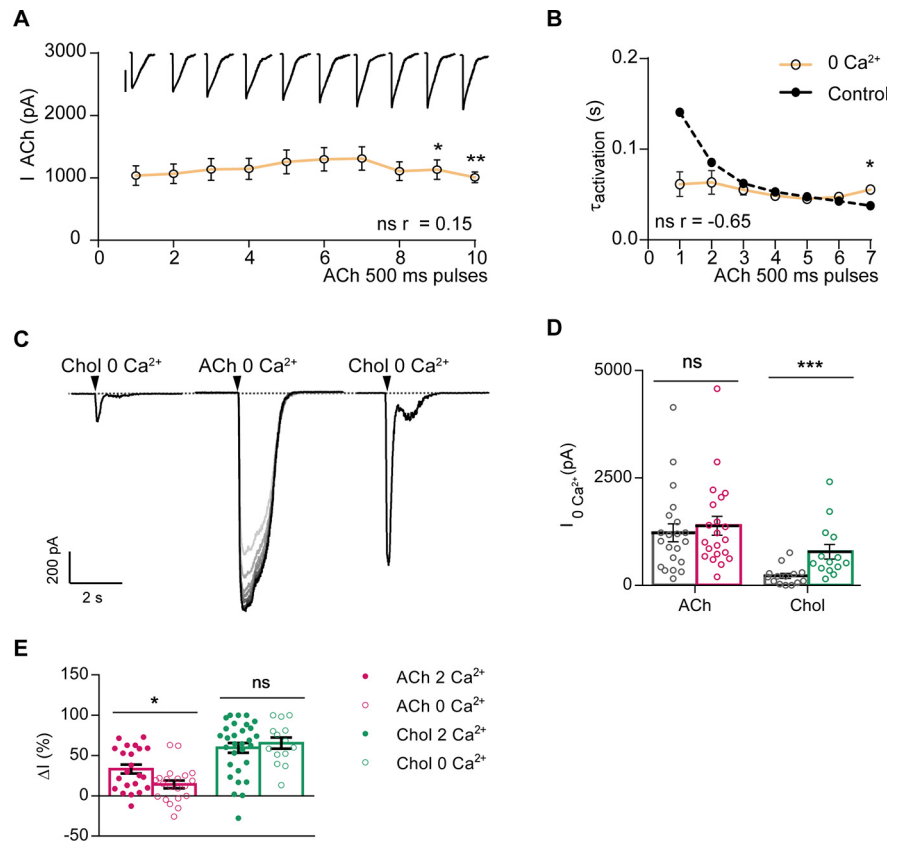


Figure 4. Dependence of Ca^{2+} of the ACh-evoked nicotinic current increment. **A**, Cells were superfused with a Ca^{2+} -free solution. The ACh peak current is drawn with respect to the number of pulses. The corresponding representative recordings for each pulse are shown in the upper part of each panel. *U* Mann–Whitney test between each data point and its equivalent point in control conditions. ACh scale: 500 pA. Choline scale: 100 pA ($n = 7–10$). **B**, Time constants of activation of the nicotinic currents from cells of panels **A**, in the seven successive ACh pulses. The dashed line represents the time constants of activation of the nicotinic currents from cells of Figure 1A, overlapped for ease of comparison. **C**, Representative recordings of the sequential application of a pulse of choline followed by seven pulses of ACh and then another choline pulse, applied every 90 s. The external solution was free of Ca^{2+} . **D**, Dot plots of the ACh and choline peak currents obtained in the absence of Ca^{2+} . Wilcoxon's test, $n = 21–23$ and $14–30$, respectively. **E**, Dot plots of the ACh ($n = 21–23$) and choline ($n = 14–30$) variation percentage in the presence and absence of Ca^{2+} . Unpaired *t* tests. Choline: chol. 2 mM Ca^{2+} : 2 Ca^{2+} . 0 mM Ca^{2+} : 0 Ca^{2+} . ACh pulses: 300 μ M, 500 ms every 90 s. Choline pulses: 3 mM, 500 ms every 90 s. * $p < 0.05$, ** $p < 0.01$, *** $p < 0.001$, ns $p > 0.05$.

The *r* Pearson's correlation coefficient achieved was 0.15 ($R^2 = 0.0212$, $p = 0.6878$; $n = 7–10$), reflecting that there is not an increase of currents with successive ACh pulses. Neither the $\tau_{activation}$ decreased with repetitive pulses ($r = -0.65$; $R^2 = 0.4299$, $p = 0.1098$), indicating that the lack of new activatable $\alpha 3\beta 4$ receptors in the absence of Ca^{2+} (see below) also affects the $\tau_{activation}$ of the whole currents (Fig. 4B). We wanted to investigate how Ca^{2+} flux through either $\alpha 7$ and $\alpha 3\beta 4$ receptors could be affecting this response. To achieve that purpose, the “potentiation protocol” was performed using an external solution free of Ca^{2+} . Representative recordings of the currents achieved under both conditions are shown in Figure 4C. The peak current elicited by choline was largely increased from 220.4 ± 58.6 to 783.4 ± 169.1 pA ($W_{(14)} = 105$, $p = 0.0001$, $n = 14$). However, the ACh increase of peak currents did not occur in a Ca^{2+} -free solution, changing from 1223 ± 208.9 to 1387 ± 217.6 pA ($W_{(21)} = 146$, $p = 0.5213$, $n = 21$). The average values of the peak currents elicited by ACh and choline are shown in Figure 4D. Also, the percentages of peak current increments elicited by both agonists are drawn in Figure 4E. They amounted to $33.3 \pm 5.6\%$ and $4.2 \pm 5\%$ for ACh in the presence and absence of Ca^{2+} , respectively ($t_{(41)} = 2.577$, $p = 0.0136$, $n = 21–23$), and to $59.61 \pm 6.3\%$

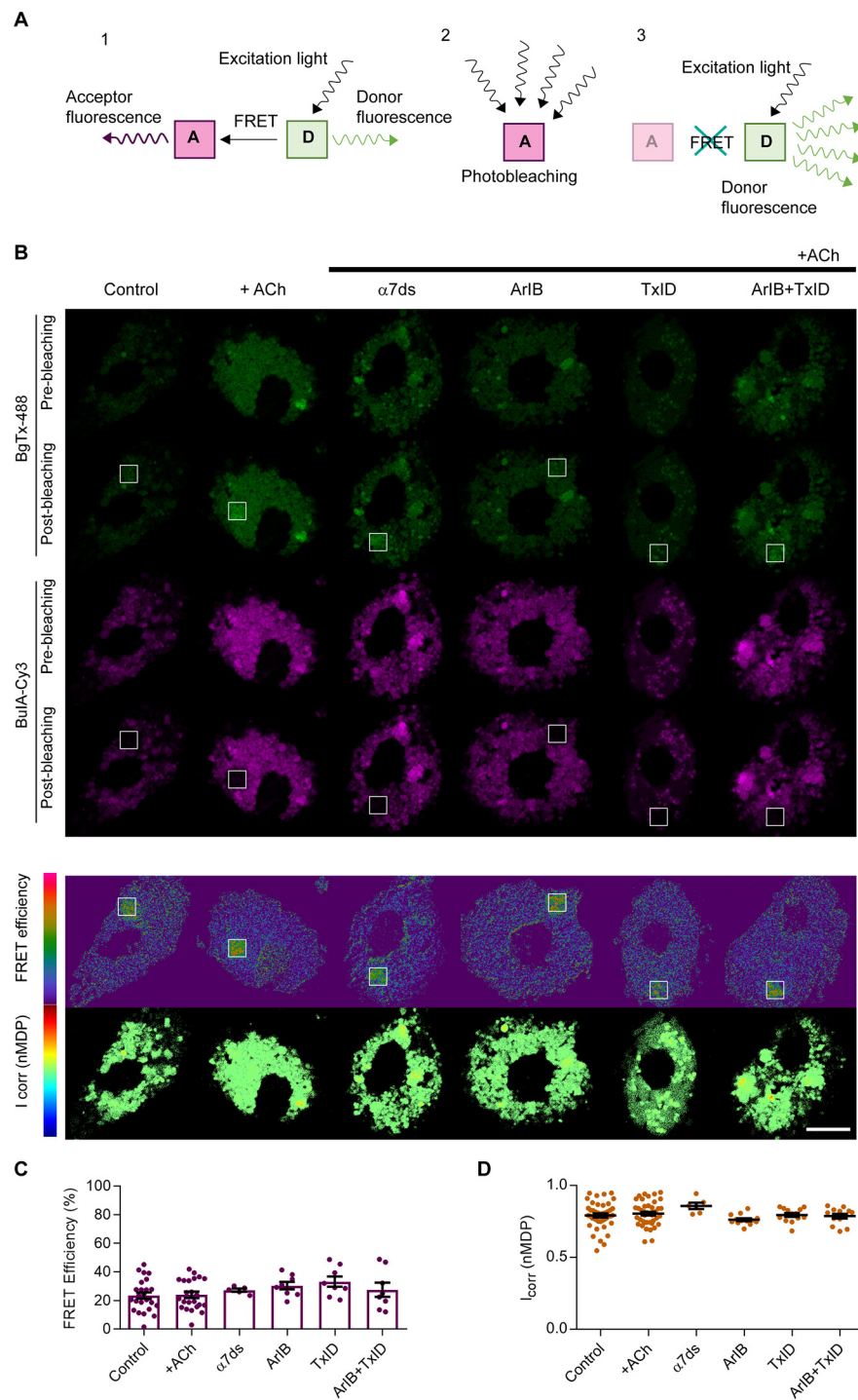


Figure 5. $\alpha 7$ and $\alpha 3\beta 4$ receptors are physically interacting: desensitization and block of $\alpha 7$ nAChR subtypes. **A**, Scheme of the FRET technique. FRET is a nonradiative transfer of an excited state from one fluorophore (donor) to another (acceptor). FRET occurs if the donor and acceptor are at a distance of 1–10 nm. In the AB technique, selective photobleaching of the acceptor causes an increase in donor emission that can be readily quantified. **B**, Representative fluorescence images of BgTx-488 and BuIA-Cy3 before and after photobleaching of the acceptor were performed, FRET efficiency, and correlation index (nMDP). The FRET AB protocol was applied to cells treated with BgTx-488 or BuIA-Cy3, under different experimental conditions: control, seven successive ACh pulses applied every 90 s, desensitizing previously the $\alpha 7$ receptor, and after treatment with Ar1B, TxID, or both toxins together. **C**, **D**, Dot plots of the corresponding percentage of FRET efficiencies ($n = 5–25$; **C**) and correlation index values (I_{corr} ; $n = 6–43$; **D**) of each cell value with respect to its control. Unpaired *t* test.

and $65.5 \pm 7\%$ for choline in the presence and absence of Ca^{2+} , respectively ($t_{(42)} = 0.581$, $p = 0.5643$, $n = 14–30$). These experiments prove that Ca^{2+} is a requirement for $\alpha 3\beta 4$ receptors to increase their flux of current but not for $\alpha 7$ receptors.

$\alpha 7$ and $\alpha 3\beta 4$ receptors are physically interacting

The functional interaction above described for $\alpha 7$ and $\alpha 3\beta 4$ receptors might be derived from a possible physical interaction. This was investigated in the present study in human chromaffin cells by FRET. The scheme of this protocol is shown in Figure 5A. We used BuIA-Cy3 as an acceptor and BgTx-488 as a donor to perform these experiments. In Figure 5B, the fluorescence images obtained under prebleaching and postbleaching conditions for the donor and the acceptor, the FRET efficiency, and the correlation index values measured as normalized mean deviation product (nMDP) are shown. Dot plots of the percentage of the FRET efficiency, calculated as explained in Materials and Methods, and the nMDP, are drawn in Figure 5C, D, respectively. Without any treatment, FRET efficiency was high, amounting to $23.3 \pm 1.3\%$ ($n = 25$), which suggests that, in human chromaffin cells, $\alpha 7$ and $\alpha 3\beta 4$ are physically interacting. The FRET efficiency was the same with the different treatments after seven successive pulses of ACh, desensitizing previously the $\alpha 7$ receptor, or treating previously the cells with Ar1B, TxID, or both toxins together (22.6–26.4%, $n = 5–23$; Table 1). Accordingly, the nMDP values obtained for the colocalization between $\alpha 7$ and $\alpha 3\beta 4$ receptors varied between 0.76 and 0.85 under these conditions ($n = 6–43$), showing a high degree of colocalization (Table 1).

Also, the efficiency of the interaction did not vary when the agonists ACh or choline were applied in the absence of Ca^{2+} , showing that Ca^{2+} does not modulate the physical interaction. Values were $30.1 \pm 4.6\%$, $36.6 \pm 4.4\%$, $33.1 \pm 3\%$, and $33.6 \pm 7.5\%$ ($n = 6$) for ACh in 2 mM and 0 Ca^{2+} , and choline 2 mM and 0 Ca^{2+} . Representative fluorescence images obtained under prebleaching and postbleaching conditions for the donor and the acceptor, the FRET efficiency, and the correlation index values are shown in Figure 6A. Dot plots of the percentage of the FRET efficiency and the nMDP are drawn in Figure 6B,C, respectively.

Tyrosine and serine/threonine phosphatases regulate $\alpha 7$ and $\alpha 3\beta 4$ receptor expression and interaction

Phosphorylation is a common regulatory mechanism of various processes. Regulation of native nonhuman $\alpha 7$ nicotinic receptors by tyrosine kinases and phosphatases has been already reported (Charpentier et al., 2005; Cho et al., 2005). Here, we

Table 1. Physical interaction between $\alpha 7$ and $\alpha 3\beta 4$ receptor subtypes

	Control	+ ACh	$\alpha 7$ ds	ArlB	TxID	ArlB + TxID
FRET efficiency (%)	22.6 \pm 1.5	23.3 \pm 1.3	27.2 \pm 1.1	25.7 \pm 2.1	26.4 \pm 2.2	22.5 \pm 3.1
I_{corr} (nMDP)	0.82 \pm 0.02	0.85 \pm 0.01	0.79 \pm 0.05	0.76 \pm 0.03	0.80 \pm 0.02	0.80 \pm 0.02

FRET efficiencies and correlation index (I_{corr}) values obtained under the different conditions of Figure 6. Control, after application of the potentiation protocol (+ACh), or application of three pulses of choline every 90 s ($\alpha 7$ ds), ArlB, TxID, or ArlB plus TxID (perfused 5 min before ACh and then during the whole experiment) before the potentiation protocol.

investigated whether the expression and interaction of $\alpha 7$ and $\alpha 3\beta 4$ receptors are regulated by tyrosine and serine/threonine-mediated phosphorylation/dephosphorylation processes. BgTx-488 and BuIA-Cy3 were again used to record $\alpha 7$ and $\alpha 3\beta 4$ receptors expression.

First, the regulation by tyrosine kinases was investigated. Representative images of the different treatments are shown in Figure 7A. Cells were incubated for 40 min with pervanadate, a tyrosine phosphatase inhibitor, at a concentration of 50 μ M. Expression of $\alpha 7$ and of $\alpha 3\beta 4$ receptor subtypes was inhibited by 30% and 34%, respectively ($U=207$, $p=0.006$; $t_{(51)}=3.127$, $p=0.0029$, $n=26$). This inhibition could be reversed by genistein (200 μ M), an inhibitor of tyrosine kinases, incubated 10 min before and during cell treatment with pervanadate ($U=202$, $p=0.0121$ and $U=161$, $p=0.0028$ for BgTx-488 and BuIA-Cy3, respectively, $n=26$). Genistein alone did not modify the expression of $\alpha 7$ and $\alpha 3\beta 4$ receptors ($t_{(51)}=0.136$, $p=0.8926$; $t_{(47)}=1.166$, $p=0.2495$, respectively, $n=25$). Dot plots of the fold times of the integrated density of BgTx and BuIA with respect to controls are shown in Figure 7B,C.

The regulation of the efficiency of the interaction between $\alpha 7$ and $\alpha 3\beta 4$ receptors by tyrosine phosphorylation/dephosphorylation was investigated by FRET. Efficiency was decreased by 20% in cells treated with pervanadate ($t_{(56)}=2.124$, $p=0.0381$, $n=26$), and recovered in cells previously incubated with genistein ($t_{(49)}=2.858$, $p=0.0062$, $n=26$). Genistein alone did not modify the efficiency of FRET achieved under basal conditions ($t_{(54)}=0.2291$, $p=0.8196$, $n=26$). Thus, the inhibition of tyrosine phosphatases has a higher impact on the interaction than the inhibition of tyrosine kinases (Fig. 7D).

Next, we investigated whether the expression and interaction of $\alpha 7$ and $\alpha 3\beta 4$ receptors are regulated by serine/threonine-mediated phosphorylation/dephosphorylation processes. BgTx-488 and BuIA-Cy3 were again used to record $\alpha 7$ and $\alpha 3\beta 4$ receptors' expression. Representative images of the different treatments are shown in Figure 7A. First, OA, an inhibitor of serine-threonine phosphatases, was incubated for 24 h at the concentration of 5 nM. Expression of $\alpha 7$ and $\alpha 3\beta 4$ receptors was inhibited by 45% and 44.5%, respectively ($t_{(48)}=4.369$, $p<0.0001$ and $t_{(48)}=3.94$, $p=0.0003$, respectively, $n=22$; Fig. 7B,C).

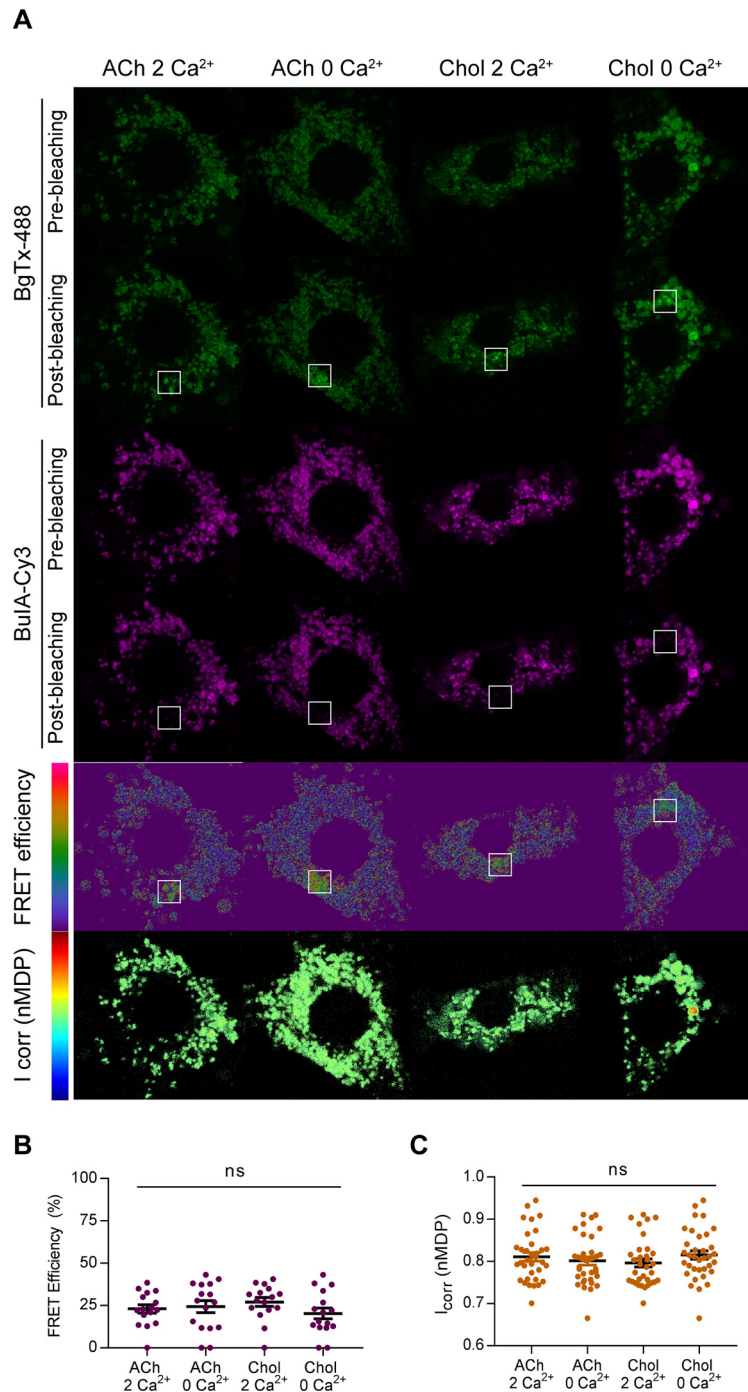


Figure 6. $\alpha 7$ and $\alpha 3\beta 4$ receptors are physically interacting: regulation by Ca^{2+} . **A**, Representative fluorescence images of BgTx-488 and BuIA-Cy3 before and after photobleaching of the acceptor were performed, FRET efficiency, and correlation index (nMDP). The FRET AB protocol was applied to cells treated with BgTx-488 or BuIA-Cy3, under different experimental conditions: ACh in 2 and 0 mM Ca^{2+} , and choline in 2 and 0 mM Ca^{2+} . **B**, **C**, Dot plots of the corresponding FRET efficiency ($n=5-25$; **B**) and correlation index values (I_{corr} ; $n=6-43$; **C**) of each cell value with respect to its control. Unpaired *t* test. ns $p>0.05$.

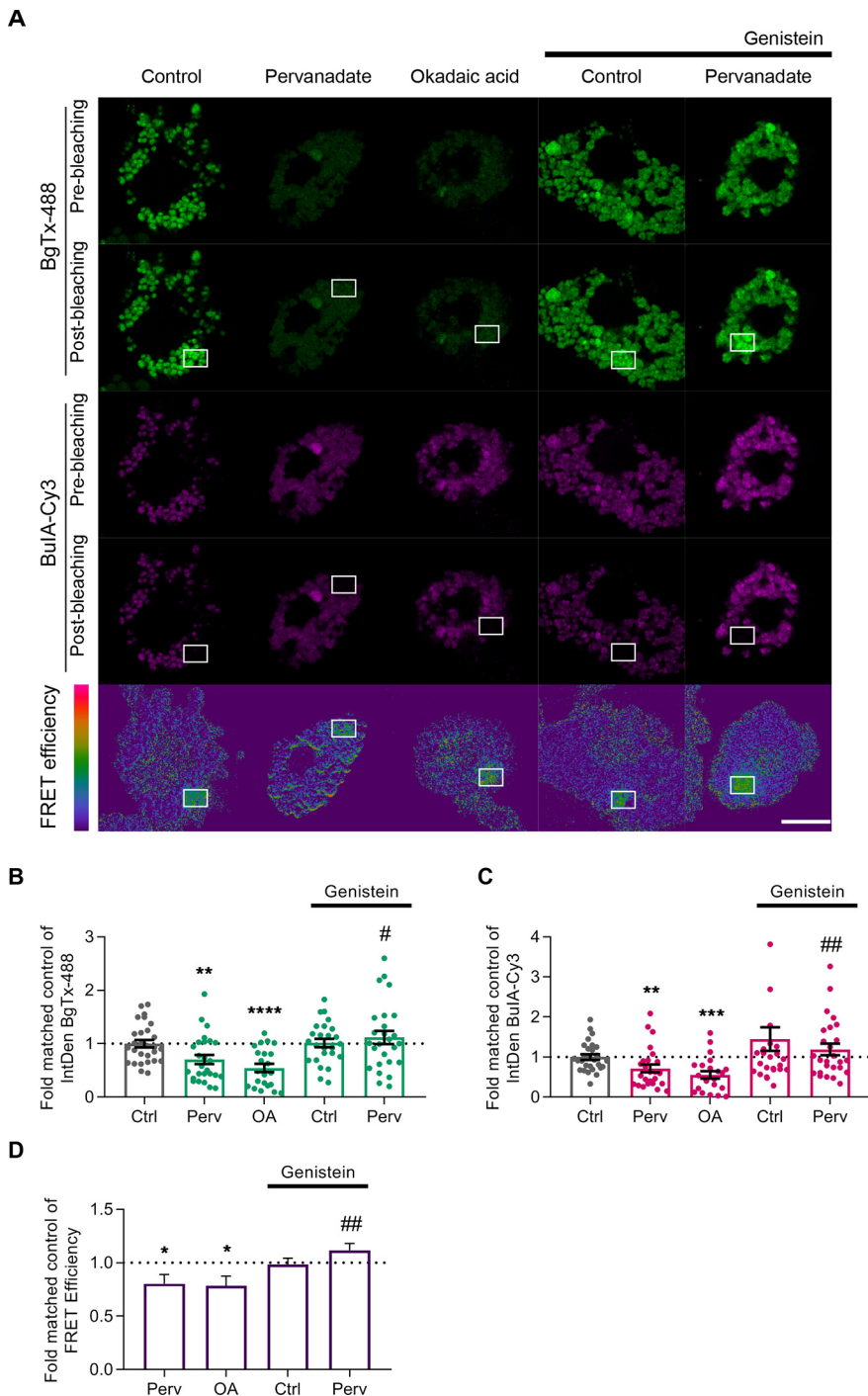


Figure 7. Tyrosine and serine/threonine phosphatases regulate $\alpha 7$ and $\alpha 3\beta 4$ receptor expression and interaction. **A**, Representative FRET images using BuIA-Cy3 as acceptor and BgTx-488 as donor. Representative fluorescence images of BgTx-488 and BuIA-Cy3 before and after photobleaching of the acceptor was performed and FRET efficiency. The FRET AB protocol was applied to cells treated with BgTx-488 or BuIA-Cy3, under different experimental conditions: control, pervanadate, genistein, OA, and genistein previously perfused to pervanadate. **B–D**, Dot plots of the fold times of the integrated density of BgTx-488 (**B**) and BuIA-Cy3 (**C**), and FRET efficiency (**D**) of each cell value calculated with respect to its control ($n = 22–26$). Unpaired t test. Perv: pervanadate. OA: okadaic acid; *differences with respect to control; #differences with respect to pervanadate. $^{*}p < 0.05$, $^{##}p < 0.01$, $^{***}p < 0.001$, $^{****}p < 0.0001$.

The efficiency of the interaction of $\alpha 7$ and $\alpha 3\beta 4$ receptors was also investigated in cells incubated with OA, obtaining a significant decrease ($t_{(52)} = 2.333$, $p = 0.0236$, $n = 22$; Fig. 7D). The values of the percentage of FRET efficiency are summarized in Table 2.

Sex dependence of the expression of $\alpha 7$ and $\alpha 3\beta 4$ receptor subtypes

The degree of physical interaction between $\alpha 7$ and $\alpha 3\beta 4$ receptor subtypes was investigated by comparing FRET efficiency in donors sorted by sex. BuIA-Cy3 and BgTx-488 were again used as acceptor and donor, respectively, in the FRET experiments. FRET efficiency did not vary between males ($23.3 \pm 1.6\%$, $n = 18$) and females ($23.1 \pm 2.4\%$, $n = 18$; $t_{(34)} = 0.0852$, $p = 0.9326$). Representative images are shown in Figure 8A. However, expression of $\alpha 7$ and $\alpha 3\beta 4$ receptor subtypes was larger in men when compared with women (Fig. 8B). Total BgTx fluorescence amounted to 323.5 ± 50.5 ($n = 16$) in males, and to 75 ± 12.6 ($n = 27$) in females ($U = 87$, $p < 0.0001$). Also, total BuIA fluorescence amounted to 194.7 ± 21.5 ($n = 16$) in males, and to 93.3 ± 13 ($n = 27$) in females ($U = 95$, $p < 0.0001$). Therefore, men express a significantly larger number of $\alpha 7$ (4.3-fold) and $\alpha 3\beta 4$ (2.1-fold) nicotinic receptors than women in human chromaffin cells.

Discussion

Multiple nAChR subtypes are expressed in the various areas of the central and peripheral nervous systems. The finality of that coexpression is not fully understood, but it might happen that these receptors are cooperating to modulate their function, which is highly dependent on the kinetics of the receptor. nAChRs exhibit a very high rate of desensitization, mainly the $\alpha 7$ subtype. Therefore, the goal of the present study was to investigate the functional cross talk between human native $\alpha 7$ and non- $\alpha 7$ nAChR subtypes. In this study we have studied in particular the $\alpha 7$ and $\alpha 3\beta 4$ subtypes in a peripheral neuroendocrine cell, the chromaffin cell of the adrenal gland. These two receptor subtypes are also expressed in different areas of the brain such as the pineal gland, but also the hippocampus, cerebellum, and medial habenula together with other nAChR subtypes. The advantage of using this neuroendocrine cell is mainly to work in a human cell, avoiding extrapolation from other species, which in addition expresses only two receptor subtypes (Pérez-Alvarez et al., 2012a,b; Hone et al., 2015, 2017), making easier to investigate the interaction between them. In this study, we have shown by FRET that these receptors physically interact. Interaction between native nAChR subtypes has not been previously reported. However, in *Xenopus* oocytes, Criado et al. (2012) showed that stable and unstable interactions between $\alpha 7$ with $\beta 4$ or $\alpha 3$ subunits, respectively, were established among human and bovine receptor subunits.

Table 2. Regulation of the physical interaction between $\alpha 7$ and $\alpha 3\beta 4$ receptor subtypes by phosphatases

	Control	Perv	OA	Gen	Gen + Perv
FRET efficiency (%)	26.37 ± 1.6	18.81 ± 1.9	21.96 ± 2.1	23.15 ± 1.2	25.02 ± 1.6
FRET efficiency (fold-matched control)	1	0.8 ± 0.09	0.78 ± 0.09	0.98 ± 0.06	1.12 ± 0.06

Pervanadate, a tyrosine phosphatase inhibitor, was used at the concentration of 50 μM and incubated for 40 min. Genistein (200 μM), an inhibitor of tyrosine kinases, was incubated 10 min before and during cell treatment with pervanadate. OA, an inhibitor of serine-threonine phosphatases, was incubated for 24 h at the concentration of 5 nM. Perv: pervanadate. Gen: genistein. OA: okadaic acid.

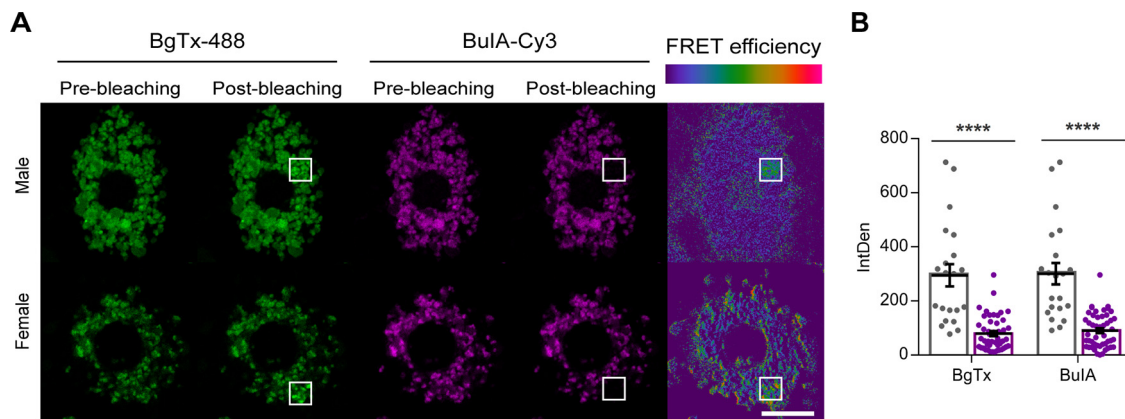


Figure 8. Sex dependence of the interaction and expression of $\alpha 7$ and $\alpha 3\beta 4$ receptor subtypes. **A**, FRET images obtained using BulA-Cy3 as acceptor and BgTx-488 as donor in chromaffin cells of male and female adrenal gland donors. **B**, Dot plots that summarize the integrated density data of BgTx-488 and BulA-Cy3, respectively, in males (gray) and females (violet; $n = 16$ from men, 27 from women). BgTx: *U* Mann–Whitney; BulA: unpaired *t* test. **** $p < 0.0001$.

Here, we have shown that after maximal efficacy of activation of $\alpha 7$ and $\alpha 3\beta 4$ nAChRs subtypes with the physiological agonist ACh, or by a synthetic agonist such as DMPP (Hone et al., 2017; Jiménez-Pompa et al., 2021), a sequence of events occurs. There is an increase of nAChR subtypes expression at the plasma membrane that are physically interacting and cooperating, and that become activatable and do not desensitize because of their mutual cooperation. These statements are proved by the following evidences: (1) enhanced expression of $\alpha 7$ and $\alpha 3\beta 4$ subtypes with repetitive pulses of ACh, which does not occur if $\alpha 7$ or $\alpha 3\beta 4$ subtypes are desensitized or blocked; (2) identical FRET efficiency achieved under control conditions and after the potentiation protocol with ACh pulses; (3) activation of a population of receptors evidenced by the associated decreased desensitization and increase of currents, because of the reciprocal cooperation between nAChR subtypes to maintain the activity of the other subtype. The $\alpha 3\beta 4$ subtype requires the $\alpha 7$ to increase their expression and activity, avoiding its desensitization, and the same occurs with the $\alpha 7$ subtype. This is a major finding of the present study that shows $\alpha 3\beta 4$ and $\alpha 7$ subtypes do not desensitize after ACh stimulation.

However, activation of these receptors with partial efficacy provokes their desensitization. This is what happens with choline, a partial agonist of $\alpha 3\beta 4$ nAChRs, and a full agonist at homomeric $\alpha 7$ receptors (Mandelzys et al., 1995; Papke et al., 1996). This agonist is obtained after degradation of ACh by the acetylcholinesterase and it is maintained at 10–20 μM in the plasma (Zeisel, 2000; Midttun et al., 2013; Cho et al., 2016; Mödinger et al., 2019). It is able to desensitize the $\alpha 7$ receptor because of its high affinity for this subtype and its low affinity for the $\alpha 3\beta 4$ receptor subtype, controlling the unlimited increase of currents elicited by ACh. However, choline will act as a brake only in the absence of ACh, otherwise, it will increase notably $\alpha 7$ receptor currents, as shown in Figure 2F. Another limiting factor

of nAChR current increase is Ca^{2+} . This cation does not affect the physical interaction between nAChR subtypes. However, our functional data reveals that the absence of Ca^{2+} avoids $\alpha 3\beta 4$, but not $\alpha 7$, nAChR currents enhancement.

The population of nAChRs that becomes activatable is not composed of new receptors, but most probably of receptors that have experienced a conformational change. This is proved by the following evidences: (1) expression of both subtypes is reversible, reduced by pervanadate, and recovered when genistein is perfused before application of the tyrosine phosphatase inhibitor; (2) increase of expression and currents occurs in a second-time scale. It has been reported that chronic exposure to a nAChR agonist such as nicotine induces an upregulation of nAChRs, not because of increased gene expression in adults. Numerous mechanisms have been proposed to be responsible for this phenomenon: increased nAChR subunit maturation and folding, increased receptor trafficking, decreased subunit degradation possibly through the pharmacological chaperoning of nAChRs by nicotine; and increased translation and second messenger signaling (Melroy-Greif et al., 2016). However, the upregulation of receptors in the present study observed is a very rapid process that occurs in a second-time scale after full activation of both receptor subtypes by the agonist.

Here, we show that physical interaction and expression of $\alpha 7$ and $\alpha 3\beta 4$ subtypes were decreased by inhibition of tyrosine or serine/threonine phosphatases. Inhibition of FRET efficiency and expression by pervanadate were reversed by genistein, reflecting that phosphorylation decreases the efficiency of the interaction and expression of nAChR subtypes. In addition, the physical interaction is reduced by OA, an inhibitor of serine/threonine phosphatase, which might be relevant if translated to the pathophysiology of AD. *In vivo* models of AD exhibit increased levels and activity of endogenous PP2A inhibitors (Tanimukai et al., 2005). The reduced activity of this enzyme, which is responsible for 70% of tau dephosphorylation activity (Liu et al., 2005), might account for hyperphosphorylation of tau

(Gong et al., 1993; Liu et al., 2005) and AD-like pathology (Gong et al., 2001; Sun et al., 2003). Furthermore, the inhibition of PP2A increases GSK-3 β activity, enhancing hyperphosphorylation of tau (Wang et al., 2015). Future work will clarify whether a dysfunction of the physical and functional interactions between nAChR subtypes might be contributing to the physiopathology of AD.

In addition, our data show that expression, but not interaction of $\alpha 7$ and $\alpha 3\beta 4$ receptors, varies with sex. Men exhibited a 2- to 3-fold increase of BgTx and BuIA receptors labeling with respect to women. It might be that the direct influence of adrenal gland steroids regulates the expression of nAChRs in the chromaffin cell. Indeed, recombinant human $\alpha 3\beta 4$ receptors are noncompetitively inhibited by estrogens (Ke and Lukas, 1996; Nakazawa and Ohno, 2001). Our data constitute the first study in which human native $\alpha 7$ and $\alpha 3\beta 4$ nicotinic receptors expression in males and females has been determined.

In summary, the present study shows that the cross talk between $\alpha 7$ and $\alpha 3\beta 4$ nAChR subtypes avoids their desensitization when these receptors are activated with maximal efficacy. In this way, repetitive ACh stimulation leads to an increase of nicotinic currents, while successive choline pulses desensitize them in the absence of ACh, controlling the unlimited rise of currents by this agonist. These data also help to identify pharmacological targets to regulate the cholinergic function, opening new perspectives for the treatment of cholinergic-related diseases.

References

- Charpentier E, Wiesner A, Huh KH, Ogier R, Hoda JC, Allaman G, Raggenbass M, Feuerbach D, Bertrand D, Fuhrer C (2005) Alpha7 neuronal nicotinic acetylcholine receptors are negatively regulated by tyrosine phosphorylation and Src-family kinases. *J Neurosci* 25:9836–9849.
- Cho CE, Taesuwan S, Malysheva OV, Bender E, Yan J, Caudill MA (2016) Choline and one-carbon metabolite response to egg, beef and fish among healthy young men: a short-term randomized clinical study. *Clin Nutr Exp* 10:1–11.
- Cho CH, Song W, Leitzell K, Teo E, Meleth AD, Quick MW, Lester RA (2005) Rapid upregulation of $\alpha 7$ nicotinic acetylcholine receptors by tyrosine dephosphorylation. *J Neurosci* 25:3712–3723.
- Criado M, Valor LM, Mulet J, Gerber S, Sala S, Sala F (2012) Expression and functional properties of $\alpha 7$ acetylcholine nicotinic receptors are modified in the presence of other receptor subunits. *J Neurochem* 123:504–514.
- Gong CX, Singh TJ, Grundke-Iqbal I, Iqbal K (1993) Phosphoprotein phosphatase activities in Alzheimer disease brain. *J Neurochem* 61:921–927.
- Gong CX, Lidsky T, Wegiel J, Grundke-Iqbal I, Iqbal K (2001) Metabolically active rat brain slices as a model to study the regulation of protein phosphorylation in mammalian brain. *Brain Res Brain Res Protoc* 6:134–140.
- Hellenkamp B, Schmid S, Doroshenko O, Opanasyuk O, Kühnemuth R, Rezaei Adariani S, Ambrose B, Aznauryan M, Barth A, Birkedal V, Bowen ME, Chen H, Cordes T, Eilert T, Fijen C, Gebhardt C, Götz M, Gouridis G, Gratton E, Ha T, et al. (2018) Precision and accuracy of single-molecule FRET measurements—a multi-laboratory benchmark study. *Nat Methods* 15:669–676.
- Hone AJ, Ruiz M, Scadden M, Christensen S, Gajewiak J, Azam L, McIntosh JM (2013) Positional scanning mutagenesis of α -conotoxin PeIA identifies critical residues that confer potency and selectivity for $\alpha 6/\alpha 3\beta 2\beta 3$ and $\alpha 3\beta 2$ nicotinic acetylcholine receptors. *J Biol Chem* 288:25428–25439.
- Hone AJ, McIntosh JM, Azam L, Lindstrom J, Lucero L, Whiteaker P, Passas J, Blázquez J, Albillos A (2015) α -Conotoxins identify the $\alpha 3\beta 4^*$ subtype as the predominant nicotinic acetylcholine receptor expressed in human adrenal chromaffin cells. *Mol Pharmacol* 88:881–893.
- Hone AJ, Michael McIntosh J, Rueda-Ruzafa L, Passas J, de Castro-Guerín C, Blázquez J, González-Enguita C, Albillos A (2017) Therapeutic concentrations of varenicline in the presence of nicotine increase action potential firing in human adrenal chromaffin cells. *J Neurochem* 140:37–52.
- Jiménez-Pompa A, Sanz-Lázaro S, Hone AJ, Rueda-Ruzafa L, Medina-Polo J, González-Enguita C, Blázquez J, de los Ríos C, McIntosh JM, Albillos A (2021) Therapeutic concentrations of varenicline increases exocytotic release of catecholamines from human and rat adrenal chromaffin cells in the presence of nicotine. *Neuropharmacology* 195:108632.
- Ke L, Lukas RJ (1996) Effects of steroid exposure on ligand binding and functional activities of diverse nicotinic acetylcholine receptor subtypes. *J Neurochem* 67:1100–1112.
- Lindau M, Neher E (1988) Patch-clamp techniques for time-resolved capacitance measurements in single cells. *Pflugers Arch* 411:137–146.
- Liu F, Grundke-Iqbal I, Iqbal K, Gong CX (2005) Contributions of protein phosphatases PP1, PP2A, PP2B and PP5 to the regulation of tau phosphorylation. *Eur J Neurosci* 22:1942–1950.
- Luo S, Zhangsun D, Zhu X, Wu Y, Hu Y, Christensen S, Harvey PJ, Akcan M, Craik DJ, McIntosh JM (2013) Characterization of a novel α -conotoxin TxID from conus textile that potently blocks rat $\alpha 3\beta 4$ nicotinic acetylcholine receptors. *J Med Chem* 56:9655–9663.
- Mandelzys A, De Koninck P, Cooper E (1995) Agonist and toxin sensitivities of ACh-evoked currents on neurons expressing multiple nicotinic ACh receptor subunits. *J Neurophysiol* 74:1212–1221.
- Melroy-Greif WE, Stitzel JA, Ehringer MA (2016) Nicotinic acetylcholine receptors: upregulation, age-related effects and associations with drug use. *Genes Brain Behav* 15:89–107.
- Midttun Ø, Kvalheim G, Ueland PM (2013) High-throughput, low-volume, multianalyte quantification of plasma metabolites related to one-carbon metabolism using HPLC-MS/MS. *Anal Bioanal Chem* 405:2009–2017.
- Mödinger Y, Schön C, Wilhelm M, Hals P (2019) Plasma kinetics of choline and choline metabolites after a single dose of SuperbaBoost™ krill oil or choline bitartrate in healthy volunteers. *Nutrients* 11:2548.
- Nakazawa K, Ohno Y (2001) Modulation by estrogens and xenoestrogens of recombinant human neuronal nicotinic receptors. *Eur J Pharmacol* 430:175–183.
- Papke RL, Bencherif M, Lippiello P (1996) An evaluation of neuronal nicotinic acetylcholine receptor activation by quaternary nitrogen compounds indicates that choline is selective for the $\alpha 7$ subtype. *Neurosci Lett* 213:201–204.
- Pérez-Alvarez A, Albillos A (2007) Key role of the nicotinic receptor in neurotransmitter exocytosis in human chromaffin cells. *J Neurochem* 103:2281–2290.
- Pérez-Alvarez A, Hernández-Vivanco A, Caba-González JC, Albillos A (2011) Different roles attributed to Cav1 channel subtypes in spontaneous action potential firing and fine tuning of exocytosis in mouse chromaffin cells. *J Neurochem* 116:105–121.
- Pérez-Alvarez A, Hernández-Vivanco A, Alonso y Gregorio S, Tabernero A, McIntosh JM, Albillos A (2012a) Pharmacological characterization of native $\alpha 7$ nicotinic ACh receptors and their contribution to depolarization-elicited exocytosis in human chromaffin cells. *Br J Pharmacol* 165:908–921.
- Pérez-Alvarez A, Hernández-Vivanco A, McIntosh JM, Albillos A (2012b) Native $\alpha 6\beta 4^*$ nicotinic receptors control exocytosis in human chromaffin cells of the adrenal gland. *FASEB J* 26:346–354.
- Sun L, Liu SY, Zhou XW, Wang XC, Liu R, Wang Q, Wang JZ (2003) Inhibition of protein phosphatase 2A- and protein phosphatase 1-induced tau hyperphosphorylation and impairment of spatial memory retention in rats. *Neurosci* 118:1175–1182.
- Tanimukai H, Grundke-Iqbal I, Iqbal K (2005) Up-regulation of inhibitors of protein phosphatase-2A in Alzheimer's disease. *Am J Pathol* 166:1761–1771.
- Wang Y, Yang R, Gu J, Yin X, Jin N, Xie S, Wang Y, Chang H, Qian W, Shi J, Iqbal K, Gong CX, Cheng C, Liu F (2015) Cross talk between PI3K-AKT-GSK-3 β and PP2A pathways determines tau hyperphosphorylation. *Neurobiol Aging* 36:188–200.
- Whiteaker P, Christensen S, Yoshikami D, Dowell C, Watkins M, Gulyas J, Rivier J, Olivera BM, McIntosh JM (2007) Discovery, synthesis, and structure activity of a highly selective $\alpha 7$ nicotinic acetylcholine receptor antagonist. *Biochem* 46:6628–6638.
- Zeisel SH (2000) Choline: an essential nutrient for humans. *Nutrition* 16:669–671.